Molecular Physics
Vol. 00, No. 00, 10 May 2008, 1–15

RESEARCH ARTICLE

Application of h-adaptive, high order finite element method to solve radial Schrödinger equation

Zbigniew Romanowski

Interdisciplinary Centre for Materials Modelling ul. Pawinskiego 5a 02-106 Warsaw, Poland

(*Received 00 Month 200x; final version received 00 Month 200x*)

h-adaptive, high order finite element method is applied to solve second order one dimension eigenvalue problem. The finite element formulation for Lobatto basis is given, for which basis functions of arbitrary order can be constructed. The adaptive algorithm is simple, yet very efficient and straightforward to implement. The algorithm is based on the observation that the expansion coefficients of Lobatto basis functions decays rapidly. It allows evaluating the smallest eigenvalues simultaneously with the comparable accuracy for all eigenvalues. The presented algorithm is applied to solve radial Schrödinger equation with Coulomb and Woods-Saxon potential. For both potentials the convergence rate is presented. After seven adaptive iterations nine digits accuracy were obtained.

Keywords: high order finite element method; h-adaptive method; Lobatto basis functions; radial Schrödinger equation

1. Introduction

The radial Schrödinger equation

$$-\frac{1}{2}\frac{\mathrm{d}^2 P_{n,\ell}(r)}{\mathrm{d}r^2} + \Big(V(r) + \frac{\ell(\ell+1)}{2r^2}\Big)P_{n,\ell}(r) = E_{n,\ell}P_{n,\ell}(r) \tag{1}$$

with $\ell = 0, 1, 2, \ldots$ is a basic equation in atomic quantum mechanics. The function $V(r)$ is called interaction potential and $n = 1, 2, \ldots$ is an eigenvalue $E_{n,\ell}$ and eigenfunction $P_{n,\ell}(r)$ index. The solution of this equation is required in order to describe:

(1) One electron systems with spherical symmetry [1],
(2) Closed shell atom in Density Functional Theory [2].

Since Eq. (1) can be solved analytically only for very few potentials $V(r)$, the numerical algorithm must be developed.

From theory of ordinary differential equations it follows, that second order eigenvalue problem like (1) must be augmented by boundary conditions in order to obtain the solutions of the eigenvalue problem. It was proved that for two cases listed above, the eigenfunctions $P_{n,\ell}$ must fulfill zero Dirichlet boundary conditions

$$\lim_{r\to 0} P_{n,\ell}(r) = \lim_{r\to\infty} P_{n,\ell}(r) = 0 \tag{2}$$

and the domain of the Eq. (1) is infinite interval $[0, \infty)$.

ISSN: 00268976 print/ISSN 13623028 online

DOI: 10.1080/0026897YYxxxxxxxx
http://www.informaworld.com

Usually, Eq. (1) is solved by application of the one of shooting methods [3, 4], for example Numerov [5] or multi-step method [6, 7]. However, the shooting methods have one serious drawback: in order to obtain the correct eigenvalues $E_{n,\ell}$, a good initial estimate for $E_{n,\ell}$ must be provided. In order to estimate the eigenvalue $E_{n,\ell}$ some preliminary calculation must be performed. Moreover, for fixed ℓ the ordering of $E_{n,\ell}$ is based on counting of the zeroes of $P_{n,\ell}(r)$, which is equivalent to solving equation $P_{n,\ell}(r) = 0$. This problem is particularly troublesome when $P_{n,\ell}(r)$ is close to zero and numerical noise can cause difficulties.

In shooting method each eigenvalue is searched individually. Applying the multi-step version of the shooting method, where the integration step is adjusted to the searched eigenfunction, very accurate results were obtained [6, 7]. The adaptability is considerable advantage of the shooting method.

The finite element method has been successfully applied in atomic and molecular physics [8–10]. The review of finite element applications in atomic physics has been presented by Pask and Sterne [11]. The application of finite element to solve Hartree-Fock problem for an atom has also been reported [12–14]. However, in most cases the basis function of finite element method were Lagrange functions [11] or B-splines [15].

In order to apply the finite element method no initial estimate for $E_{n,\ell}$ is required, as opposed to shooting method. Furthermore, the obtained eigenvalues are already sorted in increasing order. Additionally, there exists efficient algorithms in matrix algebra [16, 17] dedicated to obtain a few lowest eigenvalues and accompanying eigenvectors. It follows that finite element method is suited well for solving problem (1). Moreover, finite element method is variational, hence the eigenvalues are always greater than the exact ones.

Each algorithm, based on finite element method, must start up from construction of mesh. Having the mesh the basis functions are built on which the finite element space is spanned where the approximated solutions are searched. In order to represent the solution well, the mesh must be properly constructed. The proper choice of the mesh is crucial to obtain accurate solution with small number of mesh elements. In order to represent the solution efficiently the mesh is adjusted, based on the approximate solution obtained for coarse mesh. For each element of the coarse mesh the error is evaluated and based on the error elements are marked for split. This procedure is called h-adaptive finite element method.

In this paper we show that the application of finite-element method with high order Lobatto basis functions provides very accurate and efficient algorithm. The h-adaptive algorithm adjust the mesh for all searched eigenfunctions simultaneously. Very few iterations are required to obtain high accuracy. The complete and ready to use numerical algorithm is presented. Moreover, all necessary information required to write the efficient program is provided.

The structure of the paper is as follows. In Section 2 the complete and ready to use numerical algorithm is derived. In Section 3 the numerical results obtained by the use of the described algorithm for Coulomb and Wood-Saxon potentials are discussed. These potentials were chosen, because the eigenvalues are known with high accuracy which permits us to estimate the error of our algorithm. In the last section the discussion of the presented results is given.

2. Galerkin Finite Element

The finite element method is a general approach to solve partial and ordinary differential equations [18–20]. The method searches the approximate solution within the polynomial space $\mathcal{S}$. The Galerkin finite element method [21] is particularly

convenient in numerical applications [22] because of the orthogonality of residual to each basis function of space $\mathcal{S}$. The space $\mathcal{S}$ is linear, has the finite dimension N and is determined by the set of basis functions $\{\phi_i\}_{i=1}^N$. Application of Galerkin finite element method to differential eigenproblem leads to generalized algebraic eigenvalue problem with sparse matrices, where the elements of matrices are defined as an integrals [23].

There are many possible choices of the finite element basis functions $\{\phi_i\}$ when eigenproblem in one dimension is solved. However, in this paper Lobatto basis functions [18] are considered only. The Lobatto basis functions are applied when one dimensional eigenproblem on finite interval $[a, b] \subset \mathbb{R}$ is defined.

In finite element method, in order to build the polynomial space $\mathcal{S}$, where the approximate solutions are searched, the following steps must be made [19, 20]:

- Interval $[a, b]$ must be triangulated.
- Reference basis functions $\{\psi_i\}$ on the reference interval must be chosen (Lobatto functions in our case).
- Based on the reference functions $\{\psi_i\}$, the basis functions $\{\phi_i\}_{i=1}^N$ are constructed.

The triangulation of interval $[a, b]$ is accomplished in two steps:

- Create the sequence of points $a = x_0 < x_1 < \ldots < x_M = b$ and create set of intervals $[x_{m-1}, x_m]$ for $m = 1, \ldots, M$, where M is the number of intervals.
- For each interval $[x_{m-1}, x_m]$ assign the integer number $p_m \geq 1$, called the order of m-th interval.

In the following section the Lobatto basis functions $\{\psi_i\}$ and construction of basis functions $\{\phi_i\}_{i=1}^N$ are described.

2.1. *Lobatto basis functions*

Lobatto basis functions $\{\psi_i(s)\}$ are defined on the reference interval $s \in [-1, 1]$. By definition [18] we have

$$\psi_0(s) = (1 - s)/2 \tag{3}$$

$$\psi_1(s) = (1 + s)/2 \tag{4}$$

$$\psi_k(s) = \int_{-1}^{s} \tilde{P}_{k-1}(t)\, \mathrm{d}t \qquad \text{for } k \geq 2 \tag{5}$$

where $\tilde{P}_k(t)$ is normalized Legendre polynomial [24]

$$\tilde{P}_k(t) = \frac{P_k(t)}{||P_k||} \qquad \text{with} \qquad ||P_k||^2 = \int_{-1}^{1} P_k^2(t)\, \mathrm{d}t \tag{6}$$

and

$$P_k(t) = \frac{1}{2^k} \sum_{m=1}^{\lfloor k/2 \rfloor} (-1)^m \binom{k}{m} \binom{2k - 2m}{2k} t^{k-2m}. \tag{7}$$

Based on the above equations it is straightforward to evaluate $\psi_k(s)$ of any k. Moreover, it follows from Eq. (5), that the derivative of basis function $\psi_k(s)$ is

given by

$$\psi'_k(s) = \tilde{P}_{k-1}(s). \tag{8}$$

Based on othogonality of Legendre polynomial, the important properties of Lobatto basis functions follows for $i, j \geq 2$

$$\int_{-1}^{1} \psi'_i(s)\psi'_j(s)\mathrm{d}s = \int_{-1}^{1} \tilde{P}'_{i-1}(s)\tilde{P}'_{j-1}(s)\mathrm{d}s = \delta_{i,j} \tag{9}$$

and for $j \geq 2$

$$\int_{-1}^{1} \psi'_0(s)\psi'_j(s)\mathrm{d}s = \int_{-1}^{1} \psi'_1(s)\psi'_j(s)\mathrm{d}s = 0 \tag{10}$$

and

$$\begin{aligned} \int_{-1}^{1} \psi'_0(s)\psi'_0(s)\mathrm{d}s &= \frac{1}{2} \\ \int_{-1}^{1} \psi'_0(s)\psi'_1(s)\mathrm{d}s &= -\frac{1}{2}. \end{aligned} \tag{11}$$

Let define the matrix $\mathbf{S}$ as an overlap integral between derivatives

$$\mathbf{S}_{i,j} = \int_{-1}^{1} \psi'_i(s)\psi'_j(s)\ \mathrm{d}s. \tag{12}$$

From Eqs. (9), (10), (11) it follows that for set $\{\psi_i\}_{i=1}^{p}$ we obtain

$$\mathbf{S} = \begin{bmatrix} \frac{1}{2} & -\frac{1}{2} & 0 & 0 & \cdots & 0 \\ -\frac{1}{2} & \frac{1}{2} & 0 & 0 & \cdots & 0 \\ 0 & 0 & 1 & 0 & \cdots & 0 \\ 0 & 0 & 0 & 1 & \cdots & 0 \\ \vdots & \vdots & \vdots & \vdots & \ddots & \vdots \\ 0 & 0 & 0 & 0 & \cdots & 1 \end{bmatrix}_{p\times p}. \tag{13}$$

The sparseness of the above matrix will be used later. Since the Lobatto functions are given explicitly and are polynomials it is easy to evaluate the integrals

$$\mathbf{K}_{i,j} = \int_{-1}^{1} \psi_i(s)\psi_j(s)\mathrm{d}s. \tag{14}$$

For convenience the elements of matrix $\mathbf{K}$ are provided

$$\mathbf{K} = \begin{bmatrix} \frac{2}{3} & \frac{1}{3} & \frac{-1}{\sqrt{6}} & \frac{1}{3\sqrt{10}} & 0 & 0 & 0 & 0 & 0 & 0 & 0 \\ & \frac{2}{3} & \frac{-1}{\sqrt{6}} & \frac{-1}{3\sqrt{10}} & 0 & 0 & 0 & 0 & 0 & 0 & 0 \\ & & \frac{2}{5} & 0 & \frac{-1}{5\sqrt{21}} & 0 & 0 & 0 & 0 & 0 & 0 \\ & & & \frac{2}{21} & 0 & \frac{-1}{21\sqrt{5}} & 0 & 0 & 0 & 0 & 0 \\ & & & & \frac{2}{45} & 0 & \frac{-1}{9\sqrt{77}} & 0 & 0 & 0 & 0 \\ & & & & & \frac{2}{77} & 0 & \frac{-1}{33\sqrt{13}} & 0 & 0 & 0 \\ & & & & & & \frac{2}{117} & 0 & \frac{-1}{13\sqrt{165}} & 0 & 0 \\ & & & & & & & \frac{2}{165} & 0 & \frac{-1}{15\sqrt{221}} & 0 \\ & & & & & & & & \frac{2}{221} & 0 & \frac{-1}{17\sqrt{285}} \\ & & & & & & & & & \frac{2}{285} & 0 \\ & & & & & & & & & & \frac{2}{357} \end{bmatrix} \tag{15}$$

From definition it follows that both matrices $\mathbf{S}$, $\mathbf{K}$ are symmetric, hence only upper triangular part of matrix $\mathbf{K}$ is given.

2.2. *Construction of basis functions*

The basis functions $\{\phi_i\}_{i=1}^N$ are defined for each element $[x_{m-1}, x_m]$ independently and their definition is based on Lobatto basis functions $\{\psi_i\}$ defined on the reference interval $[-1, 1]$. In order to construct basis functions $\{\phi_i\}$ on m-th element the map $h_m : [-1, 1] \to [x_{m-1}, x_m]$ is introduced

$$h_m(s) = \frac{x_m + x_{m-1}}{2} + \frac{x_m - x_{m-1}}{2} s. \tag{16}$$

Then the k-th basis function ϕ_k constructed on m-th element based on ψ_i is defined as a superposition

$$\phi_k(x) = \psi_i(h_m^{-1}(x)) \qquad \text{for} \quad i = 0, \ldots, p_m \tag{17}$$

It can be shown [18] that functions $\{\phi_k\}$ defined in the above equation constitute the basis for linear polynomial functional space $\mathcal{S}$. In Eq. (17) the index k depends on indices i and m. The index k can be arbitrarily chosen but it must be unique for pair (i, m). The indexing scheme determines the structure of the matrices defined in Section 2.3 and hence has great impact on numerical performance. In our algorithm the following indexing scheme is applied.

(1) Indexing starts from left interval $m = 1$ and runs to right interval $m = M$.
(2) Since zero Dirichlet boundary conditions are applied, the basis on most-left element $m = 1$ and most-right element $m = M$ are skipped.
(3) $k = 0$. For each element m of degree p_m

- If $p_m > 1$, then index k is incremented for each basis function ψ_p for $p = 2, \ldots, p_m$.
- Before going to the next element index k is decremented in order to mach linear basis functions from adjacent intervals.

Based on the above scheme it is straightforward to determine the dimension N of the polynomial space $\mathcal{S}$

$$N = \underbrace{M-1}_{\text{I}} + \underbrace{\sum_{m=1}^{M}(p_m-1)}_{\text{II}} = \sum_{m=1}^{M} p_m - 1. \tag{18}$$

The term I includes the basis functions of first order and the term II includes the basis functions of higher orders. Further, this indexing scheme is used to determine the structure of matrices $\mathbf{A}$, $\mathbf{Q}$ discussed in Section 2.3. The indexing scheme described above leads to banded matrices $\mathbf{A}$ and $\mathbf{Q}$.

2.3. *Second order eigenproblem*

In this Section the algorithm of the approximate solution of the eigenproblem

$$-\gamma\, y''(x) + g(x)y(x) = \lambda y(x) \qquad \gamma \in \mathbb{R} \tag{19}$$

is provided. We search a few lowest eigenvalues λ and the associated eigenfunctions $y(x)$. The eigenfunctions $y(x)$ are defined on a finite interval $[a,b]$ and must fulfill Dirichlet zero boundary conditions: $y(a) = y(b) = 0$. Let create the space $\mathcal{S}$ spanned on the basis $\{\phi_i\}_{i=0}^{N}$ described in previous sections. We search the approximate solution of eigenfunction in the space $\mathcal{S}$:

$$y(x) \approx \tilde{y}(x) = \sum_{i=1}^{N} c_i \phi_i(x). \tag{20}$$

Additionally, $\tilde{y}(x)$ must fulfill Dirichlet zero boundary conditions: $\tilde{y}(a) = \tilde{y}(b) = 0$. In order to calculate the coefficients, $\{c_i\}$, Galerkin finite element method [21, 22, 25] is applied. Let substitute the approximate function from Eq. (20) into Eq. (19):

$$R(\{c_i\}, x) = -\gamma \sum_{i=1}^{N} c_i \phi_i''(x) + [g(x) - \lambda] \sum_{i=1}^{N} c_i \phi_i(x) \tag{21}$$

where $R(\{c_i\}, x)$ is a residual. According to Galerkin method, the residual must be orthogonal to each basis function (in our case ϕ_j):

$$\int_a^b R(\{c_i\}, x)\phi_j(x)\,\mathrm{d}x = 0 \qquad \text{for} \qquad j = 1, \ldots, N. \tag{22}$$

Substituting Eq. (21) into Eq. (22) we get, for $j = 1, \ldots, N$:

$$-\gamma \sum_{i=1}^{N} c_i \int_a^b \phi_i''(x)\phi_j(x)\mathrm{d}x + \sum_{i=1}^{N} c_i \int_a^b g(x)\phi_i(x)\phi_j(x)\mathrm{d}x = \lambda \sum_{i=1}^{N} c_i \int_a^b \phi_i(x)\phi_j(x)\mathrm{d}x. \tag{23}$$

Using the properties of basis functions $\phi_i(a) = \phi_i(b) = 0$ (valid for $i = 1, \ldots, N$), the integral $\int_a^b \phi_i''(x)\phi_j(x)\mathrm{d}x$ can be evaluated integrating by parts

$$\int_a^b \phi_i''(x)\phi_j(x)\mathrm{d}x = -\int_a^b \phi_i'(x)\phi_j'(x)\mathrm{d}x \tag{24}$$

Using equation (24), equation (23) can be rewritten in the matrix form:

$$\mathbf{A}\boldsymbol{c} = \lambda\mathbf{Q}\boldsymbol{c} \qquad \text{with} \qquad \boldsymbol{c} = [c_1, \ldots, c_N]^T. \tag{25}$$

The matrix elements are defined as

$$\mathbf{A}_{i,j} = \mathbf{F}_{i,j} + \mathbf{G}_{i,j} \tag{26}$$

where

$$\mathbf{F}_{i,j} = \gamma \int_a^b \phi_i'(x)\phi_j'(x)\mathrm{d}x = \gamma \sum_{m=1}^{M} \int_{x_{m-1}}^{x_m} \phi_i'(x)\phi_j'(x)\mathrm{d}x \tag{27}$$

$$\mathbf{G}_{i,j} = \int_a^b g(x)\phi_i(x)\phi_j(x)\mathrm{d}x = \sum_{m=1}^{M} \int_{x_{m-1}}^{x_m} g(x)\phi_i(x)\phi_j(x)\mathrm{d}x \tag{28}$$

$$\mathbf{Q}_{i,j} = \int_a^b \phi_i(x)\phi_j(x)\mathrm{d}x = \sum_{m=1}^{M} \int_{x_{m-1}}^{x_m} \phi_i(x)\phi_j(x)\mathrm{d}x \tag{29}$$

Moreover, for Lobatto basis functions some above integrals can be further simplified. Let first consider integral in Eq. (27). Let us apply the substitution $x = h_m(s)$, where mapping h_m is defined by Eq. (16). Since

$$J_m \equiv h_m'(s) = (x_m - x_{m-1})/2 \tag{30}$$

is independent on variable s, then we obtain

$$\int_{x_{m-1}}^{x_m} \phi_i'(x)\phi_j'(x)\ \mathrm{d}x = J_m \int_{-1}^{1} \phi_i'(h_m^{-1}(s))\ \phi_j'(h_m^{-1}(s))\ \mathrm{d}s \tag{31}$$

$$= J_m \int_{-1}^{1} \psi_i'(s)\psi_j'(s)\ \mathrm{d}s = J_m \mathbf{S}_{i,j}. \tag{32}$$

Similarly one obtains

$$\int_{x_{m-1}}^{x_m} \phi_i(x)\phi_j(x)\ \mathrm{d}x = J_m \mathbf{K}_{i,j}. \tag{33}$$

It follows that matrices $\mathbf{F}$ and $\mathbf{Q}$ can be evaluated analytically. The elements of matrix $\mathbf{G}$ can be calculated using Gaussian quadratures [3]. Moreover, the matrices $\mathbf{A}$ and $\mathbf{Q}$ have the following properties:

- $\mathbf{A}$ and $\mathbf{Q}$ are square, symmetric matrices of the size $N \times N$.
- $\mathbf{Q}$ is positive definite [3].
- Since the support of ϕ_i and hence ϕ_i' is the finite interval, the matrices $\mathbf{A}$ and $\mathbf{Q}$ are sparse.

- Because of the indexing scheme presented in Section 2.2 the matrices **A**, **Q** are banded.

It shows that using Galerkin finite element method with space $\mathcal{S}$ the functional eigenproblem, Eq. (19), is reduced to algebraic generalized symmetric positive-definite eigenproblem, Eq. (25), with banded matrices **A** and **Q**. There exists efficient algorithm, finding a few lowest eigenvalues and associated eigenvectors for this problem and is implemented in LAPACK [16] library as `dsbgvx` procedure.

2.4. *h-adaptive algorithm*

In this section the adaptive algorithm is presented. The algorithm is simple, yet very efficient and straightforward to implement. The algorithm is based on the observation that the expansion coefficients of Lobatto basis functions decays rapidly. It allows evaluating the smallest eigenvalues simultaneously with the accuracy comparable for all eigenvalues.

Let us consider the mesh $\mathcal{T}$. Based on this mesh $\mathcal{T}$ let us evaluate a few smallest eigenvalues and corresponding eigenvectors applying the algorithm described in previous Sections. Since the algorithm is based on the finite element method the components of eigenvectors are the expansion coefficients in Lobatto basis functions. For each eigenvector i and for each element e of mesh $\mathcal{T}$, the smallest expansion coefficient can be found. Let denote this coefficient as $c_{i,\mathrm{e}}$. Out of these components $\{c_{i,\mathrm{e}}\}$, for given i, the largest coefficient

$$c_i^* = \max_{\mathrm{e}\in\mathcal{T}} \{|c_{i,\mathrm{e}}|\} \tag{34}$$

is identified. Since the mesh $\mathcal{T}$ is finite, then for each eigenvalue i there exists element $\mathrm{e}_i^* \in \mathcal{T}$ corresponding to the coefficient c_i^*. In our algorithm all elements e_i^* for all i are marked to split. Each marked element is split into two halves and new mesh $\mathcal{T}'$ is obtained. The calculations are repeated for new mesh $\mathcal{T}'$. The adaptive loop is repeated until coefficients c_i^* are less than prescribed value.

From the above description it is clear that for each adaptive iteration no more than P element splits are made, where P is the number of searched eigenvalues. Further, if the order of applied Lobatto basis function is Q, then the performed splits increase the dimension of the finite element method by no more than $P \times Q$. However, from our extended numerical experiments we observed that very often the coefficients c_i^* and c_j^* for $i \neq j$ corresponds to the same element, $\mathrm{e}_i^* = \mathrm{e}_j^*$. Hence, the dimension of the finite element space increases rather slowly.

The dimension increase of the finite element space is demonstrated on Figs. 1-6. On these diagrams the top horizontal axis denotes the dimension of the finite element space. From these examples it follows that in average one or two elements are split only when four smallest eigenvalues are determined.

2.5. *Truncation error*

Let us consider the case when the eigenvalue problem (1) is defined on the infinite interval $[0, \infty)$. Since the algorithm described in previous sections is formulated for finite interval only, the infinite interval $[0, \infty)$ must be replaced by finite interval $[0, R_{\max}]$. It is evident that this process introduces an error, which is called truncation error and denoted by δ in the following of the manuscript. Below, we describe the simple recipe how to control the truncation error δ.

Let assume that the eigenfunction $P_{n,\ell}(r)$ satisfy zero Dirichlet boundary condi-

tion at infinity

$$\lim_{r\to\infty} P_{n,\ell}(r) = 0 \tag{35}$$

Moreover, from the physical interpretation of eigenfunctions $P_{n,\ell}(r)$ it follows that the integral

$$\int_0^\infty r^2 P_{n,\ell}^2(r)\mathrm{d}r < \infty \tag{36}$$

is finite. Hence, for each $\delta^* > 0$, there exists $R_{\max} > 0$ that fulfills the condition

$$\int_{R_{\max}}^\infty r^2 P_{n,\ell}^2(r)\mathrm{d}r < \delta^*. \tag{37}$$

Let consider the mesh $\mathcal{T}$ for the interval $[0, R_{\max}]$. Let solve the problem (1) for this mesh $\mathcal{T}$ applying the above algorithm. For each eigenvalue n let denote by $\mathbf{d}_n$ the expansion coefficients corresponding to the right-most element i.e. close to $R_{\max}$. In our algorithm the truncation error δ_n for n-th eigenvalue is approximated as a norm of vector $\mathbf{d}_n$

$$\delta_n = |\mathbf{d}_n|. \tag{38}$$

In particular we used absolute norm of the vector $\mathbf{d}_n$

$$\delta_n = \sum_j |d_{n,j}|. \tag{39}$$

From quantum chemistry it follows that for $n > m$ the eigenfunction $P_{n,\ell}(r)$ is more diffuse than $P_{m,\ell}(r)$. Hence, we expect $\delta_n \geq \delta_m$. In order to keep the number of parameters as small as possible we introduce

$$\delta = \max_n \{\delta_n\}. \tag{40}$$

The parameter δ is an input parameter to our algorithm and is called the truncation error.

3. Numerical results

The algorithm described in previous Sections has been implemented in program `RSchrRad`. The program solves Eq. (19) with $\gamma = 1/2$ and for various functions $g(x)$. In this section we provide the numerical results obtained by this program with

$$g(r) = V(r) + \frac{\ell(\ell+1)}{2r^2}, \tag{41}$$

where $V(r)$ is an interaction potential. The efficiency and accuracy of the procedure is demonstrated for Coulomb potential and Woods-Saxon potential. The obtained results are compared with the results available in the literature. Lobatto basis function of order $Q = 6$ were applied to all elements in the mesh and the truncation error was set to $\delta = 10^{-7}$.

3.1. *Hydrogen atom*

In this section the results for Coulomb potential $V(r) = -1/r$ are presented. For this potential the analytical results are well known [1]

$$E_{n,\ell} = -\frac{1}{2(n+\ell)^2}. \tag{42}$$

Key aspect of the adaptive algorithm is convergence rate, which can be measured as a number of iterations, required to obtain the specific accuracy. Since each adaptive step increases the dimension of the finite element space, this parameter is also given.

Let us denote by $E_{\rm num}$ numerical results and by E analytical eigenvalues. In Figs. 1-3 the difference $E_{\rm num} - E$ is presented for $\ell = 0, 1, 2$, respectively. For each ℓ four smallest eigenvalues were calculated. For $\ell = 0, 1, 2$, the radial Schrödinger equation on the interval $r \in [0, 150]$, $r \in [0, 200]$, $r \in [0, 300]$ was solved, respectively. These intervals corresponds to truncation error $\delta < 10^{-7}$. The intervals are quite large, which is caused by diffuse eigenfunction for $n = 4$. However, as it follows from Figs. 1-3, the large intervals are efficiently handled by the present algorithm. The accuracy of 10 significant digits was obtained after 7 adaptive steps. This correspond to $N = 83, 83, 77$, for $\ell = 0, 1, 2$, respectively. Hence, the dimension of the arrays in generalized algebraic eigenvalue problem (25) is small. Moreover, the convergence rate is nearly exponential, which is demonstrated by almost straight line in the logarithmic scale in Figs. 1-3. Furthermore, $(E_{\rm num} - E) > 0$, hence the numerical implementation is variational, as stems from the theoretical formulation of the finite element method.

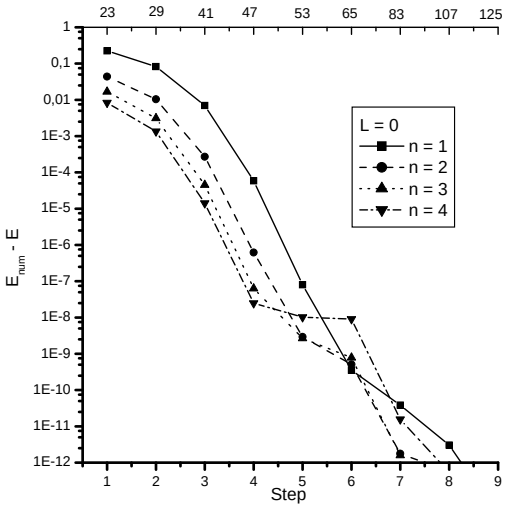

Figure 1. The difference $E_{\rm num} - E$ for each adaptive step for Coulomb potential with $\ell = 0$. The eigenvalues were obtained on interval $r \in [0, 150]$. Top horizontal axis denotes the dimension of the finite element space.

3.2. *Woods-Saxon potential*

In this Section the eigenvalues obtained for Woods-Saxon potential [26–30] for $\gamma = 1$ and

$$V(r) = \frac{u_0}{1+t} + \frac{u_1 t}{(1+t)^2}, \qquad t = \exp\left(\frac{r - r_0}{a}\right) \tag{43}$$

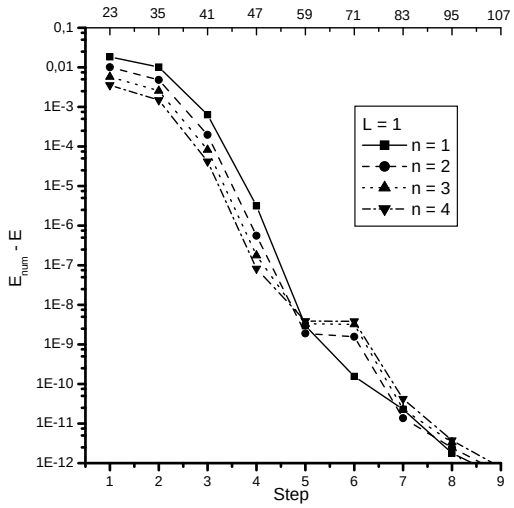

Figure 2. The difference $E_{\rm num}-E$ for each adaptive step for Coulomb potential with $\ell = 1$. The eigenvalues were obtained on interval $r \in [0, 200]$. Top horizontal axis denotes the dimension of the finite element space.

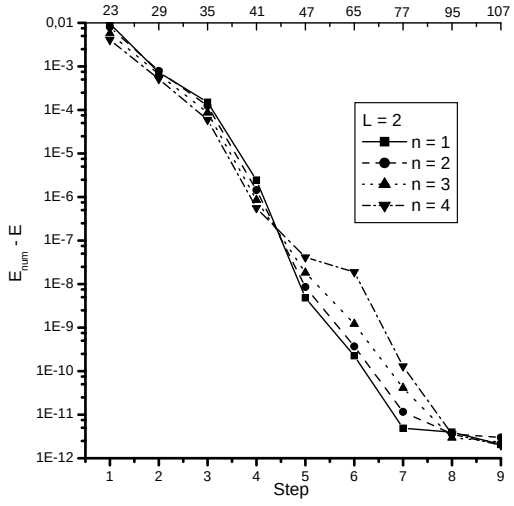

Figure 3. The difference $E_{\rm num}-E$ for each adaptive step for Coulomb potential with $\ell = 2$. The eigenvalues were obtained on interval $r \in [0, 300]$. Fitting the straight line to curve in logarithmic scale for $n = 1$ we obtained the slope coefficient about (-3.2). Top horizontal axis denotes the dimension of the finite element space.

are presented. The numerical results were obtained with parameters $u_0 = -50$, $u_1 = -u_0/a$, $a = 0.6$, $r_0 = 7$. As for hydrogen atom, the difference $|E_{\rm num} - E|$ is analyzed. However, for Woods-Saxon potential the analytical results i.e. exact eigenvalues are not known. As a reference values the numerical results with 9 digits accuracy, obtained by Vanden Berghe [26], were taken. In Figs. 4-6 the difference $|E_{\rm num} - E|$ for $\ell = 0, 1, 2$ is presented, respectively. For the above listed values of u_0, u_1, a, r_0 the eigenfunctions are not diffuse and the domain $r \in [0, 20]$ is sufficient to obtain the eigenfunctions with the truncation error $\delta < 10^{-7}$.

As for Coulomb potential, the convergence rate is fast and the dimension of the finite element space is small. However, since the reference eigenvalue E has only 9 digit of accuracy, the difference $|E_{\rm num} - E|$ does not have to converge to 0 as is shown by almost horizontal line in Fig. 4 for $n = 1$. For this case, we believe that our results approximate exact values better and 10th digit in reference eigenvalue E is not correct, hence the difference $|E_{\rm num} - E|$ is almost constant when increasing the number of adaptive steps. The similar situation is observed in Fig. 5 for $\ell = 1$

and $n = 1$. Moreover, the convergence is fast, almost exponential.

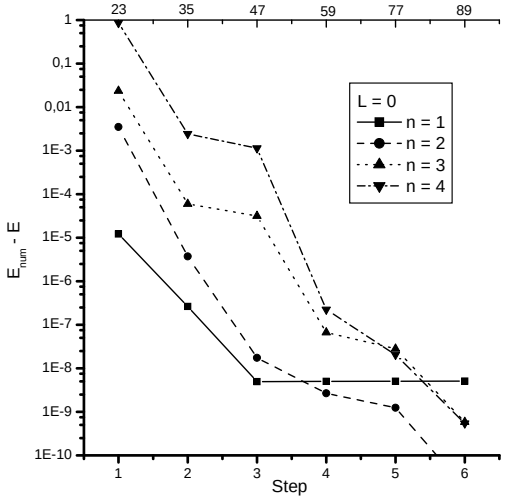

Figure 4. The difference $E_{\text{num}} - E$ for each adaptive step for Woods-Saxon potential with $\ell = 0$. The eigenvalues were obtained on interval $r \in [0, 20]$. Top horizontal axis denotes the dimension of the finite element space.

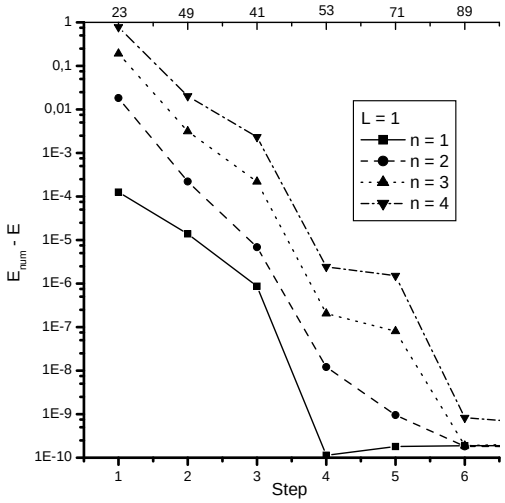

Figure 5. The difference $E_{\text{num}} - E$ for each adaptive step for Woods-Saxon potential with $\ell = 1$. The eigenvalues were obtained on interval $r \in [0, 20]$. Top horizontal axis denotes the dimension of the finite element space.

4. Conclusions

The h-adaptive algorithm solving radial Schrödinger equation is described. The presented algorithm is based on Finite Element Method with high order Lobatto basis functions. The accuracy and efficiency of the algorithm is demonstrated for Coulomb and Woods-Saxon potentials. The algorithm is stable for singular Coulomb potential. It gives the accurate results for very diffuse eigenfunctions as it was demonstrated for hydrogen atom. For discussed potentials, seven adaptive steps were necessary in order to obtain four smallest eigenvalues with the error smaller than 10^{-9}.

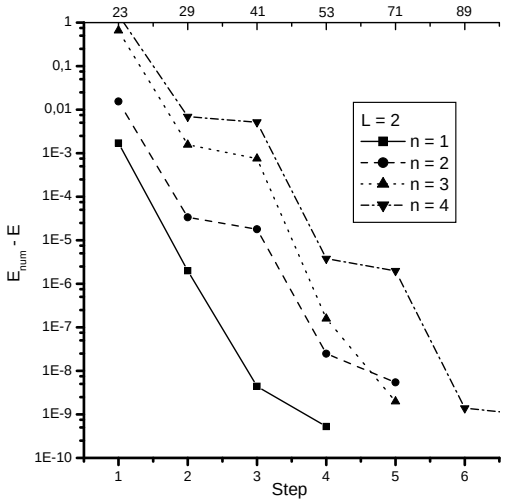

Figure 6. The difference $E_{\text{num}} - E$ for each adaptive step for Woods-Saxon potential with $\ell = 2$. The eigenvalues were obtained on interval $r \in [0, 20]$. Top horizontal axis denotes the dimension of the finite element space.

The algorithm is general and can be applied to any second order one dimensional eigenvalue problem. Furthermore, the straightforward estimate of truncation error is presented, when the eigenvalue problem is defined on infinite interval and has to be replaced by the finite domain.

4.1. *Possible applications*

In the present paper, the efficient, adaptive method solving the radial Schrödinger equation has been presented. The method is general and very stable. One of the possible application of the presented algorithm is the solution of non-linear Kohn-Sham eigenvalue problem [2] for free or confined atom. It is expected, that the application of adaptive algorithm will lead to very accurate results, serving as a reference values for various approximations for correlation and exchange energy.

A second possible application of the algorithm is the generation of pseudo-potentials [31–33] and effective core potentials required for efficient solution of Kohn-Sham equation for molecular or periodic systems.

The above listed two problems can be solved by direct application of the discussed algorithm. A third, and the most involved application, is not so closely related. One of the most successful approach to solve Kohn-Sham eigenproblem for molecular systems is based on the Linear Combinations of Atomic Orbitals (LCAO) [34, 35]. In order to evaluate the obtained integrals within the DFT-LCAO framework, the GTOs or STOs are usually applied as an atomic orbitals [2]. The radial parts of GTO and STO is proportional to $\exp(-\alpha_i r^2)$ and $\exp(-\alpha_i r)$, respectively, where $\{\alpha_i\}$ is a set of parameters characteristic for applied basis set and could be different for various systems. Based on the variational principle, in order to obtain high accuracy results, the set of parameters $\{\alpha_i\}$ should be optimized for any studied system. However, the parameter optimization is seldom done, because of high non-linearity of obtained system of equations [36–38].

These non-linear optimization problem could be completely avoided, if the radial part of atomic orbital would be represented as a linear combination of polynomial basis functions, for example basis function constructed on Lobatto polynomials, as discussed in Section 2.2. In the present paper, it was shown that application of these basis functions leads to very hight accuracy for specific one-dimensional problem. Additionally, the h-adaptive algorithm was proposed, analogous to optimization of

parameter set $\{\alpha_i\}$, however, much more straightforward to implement. In order to develop complete algorithm able to solve Kohn-Sham eigenproble for molecular system, further research is needed. One o the problem that must be solved is the evaluation of one-electron integrals (analytically or numerically), what will be reported in the separate paper.

References

[1] R.L. Liboff, *Introductory Quantum Mechanics* (Addison Wesley, New York, 1987).
[2] W. Koch and M.C. Holthausen, *A Chemist's Guide to Density Functional Theory* (Wiley, New York, 2000).
[3] J. Stoer and R. Bulirsch, *Introduction to Numerical Analysis* (Springer, New York, 2004).
[4] J. Cooley, An improved eigenvalue corrector formula for solving the Schrödinger equation for central fieldsMath. Comput. **15**, 363–374 (1961).
[5] C. Frose Fischer, T. Brage and P. Jönsson, *Computational Atomic Structure* (Institute of Physics Publishing, Bristol, 1997).
[6] L.G. Ixaru, H. De Meyer and G. Vanden Berghe, Highly accurate eigenvalues for the distorted Coulomb potentialPhys. Rev. E **61**, 3151–3159 (2000).
[7] H. Ishikawa, Numerical methods for the eigenvalue determination of second-order ordinary differential equationsJ. Comput. Appl. Math. **208**, 404–424 (2007).
[8] J.L. Gázquez and H.J. Silverstone, Piecewise polynomial electronic wavefunctionsJ. Chem. Phys. **67**, 1887–1898 (1977).
[9] S.R. White, J.W. Wilkins and M.P. Teter, Finite-element method for electronic structurePhys. Rev. B **39**, 5819–5833 (1989).
[10] J. Sapirstein and W.R. Johnson, The use of basis splines in theoretical atomic physicsJ. Phys. B: At. Mol. Phys. **29**, 5213 (1996).
[11] J.E. Pask and P.A. Sterne, Finite element methods in *ab initio* electronic structure calculationsModelling Simul. Mater. Sci. Eng. **13**, R71 (2005).
[12] C. Froese Fischer, W. Guo and Z. Shen, Spline methods for multiconfiguration Hartree-Fock calculationsInt. J. Quant. Chem. **42**, 849–867 (1992).
[13] D. Sundholm and J. Olsen, Finite-element multiconfiguration Hartree-Fock calculations of electron affinities of manganeseChem. Phys. Lett. **233**, 115–122 (1995).
[14] D. Sundholm, J. Olsen and S.A. Alexander, Finite-element multiconfiguration Hartree-Fock calculations on the excitation energies and the ionization potential of oxygenJ. Chem. Phys. **96**, 5229–5232 (1992).
[15] Z. Romanowski, B-Spline finite element solution of Kohn-Sham equation for atomModelling Simul. Mater. Sci. Eng. **16**, 015003 (2008).
[16] E. Anderson, Z. Bai, C. Bischof *et al.*, *The LAPACK Users' Guide* (SIAM, London, 1999; `http://www.netlib.org/lapack/`), `http://www.netlib.org/lapack/`.
[17] G.H. Golub and C.F. Van Loan, *Matrix Computation* (The Johns Hopkins University Press, Baltimore, 1996).
[18] P. Šolín, K. Segeth and I. Doležel, *High-Order Finite Element Method* (CHAPMAN & HALL/CRC, London, 2004).
[19] S.C. Brenner and L.R. Scott, *The Mathematical Theory of Finite Element Methods* (Springer, London, 1996).
[20] P.G. Ciarlet, *The Finite Element Method for Elliptic Problems* (North-Holland Publishing Company, Holland, 1978).
[21] C.A.J. Fletcher, *Computational Galerkin Methods* (Springer, Berlin, 1984).
[22] R. Wait and A.R. Mitchell, *Finite Element Analysis and Applications* (Wiley, New York, 1986).
[23] C. Johnson, *Numerical solution of partial differential equations by the finite element method* (Cambridge University Press, Cambridge, 1987).
[24] M. Abramowitz and I.A. Stegun, *Handbook of Mathematical Functions with Formulas, Graphs, and Mathematical Tables* (Dover Publications, New York, 1972; `http://www.math.sfu.ca/ cbm/aands/toc.htm`), `http://www.math.sfu.ca/ cbm/aands/toc.htm`.
[25] P.M. Prenter, *Splines and variational methods* (Wiley, New York, 1989).
[26] G. Vanden Berghe, V. Fack and H.E. de Meyer, Numerical methods for solving radial Schrödinger equationsJ. Comput. Appl. Math. **28**, 391–401 (1989).
[27] L.G. Ixaru and M. Rizea, A Numerov-like scheme for the numerical solution of the Schrödinger equation in the deep continuum spectrum of energiesComp. Phys. Commun. **19**, 23–27 (1980).
[28] J. Vigo-Aguiar and T.E. Simos, Review of multistep methods for the numerical solution of the radial Schrödinger equationInt. J. Quant. Chem. **103**, 278–290 (2005).
[29] L.G. Ixaru and M. Rizea, Comparison of some four-step methods for the numerical solution of the Schrödinger equationComp. Phys. Comm. **38**, 329–337 (1985).
[30] T. Simosa and P. Williams, On finite difference methods for the solution of the Schrödinger equation-Computers & Chemistry **23**, 513–554 (1999).
[31] C.J. Smallwood, R.E. Larsen, W.J. Glover and B.J. Schwartz, A computationally efficient exact pseudopotential method. I. Analytic reformulation of the Phillips-Kleinman theoryJ. Chem. Phys. **125**, 074102 (2006).
[32] M. Hodak, S. Wang, W. Lu and J. Bernholc, Implementation of ultrasoft pseudopotentials in large-scale grid-based electronic structure calculationsPhys. Rev. B **76**, 085108 (2007).

[33] M.L.T. D. Naveh, L. Kronik and J.R. Chelikowsky, Real-space pseudopotential method for spin-orbit coupling within density functional theoryPhys. Rev. B **76**, 153407 (2007).
[34] C.C.J. Roothaan, Self-Consistent Field Theory for Open Shells of Electronic SystemsRev. Mod. Phys. **32**, 179–185 (1960).
[35] ———, New Developments in Molecular Orbital TheoryRev. Mod. Phys. **23**, 69–89 (1951).
[36] K.K. T. Koga and A. Thakkar, Noninteger principal quantum numbers increase the efficiency of Slater-type basis setsInt. J. Quant. Chem. **62**, 1–11 (1997).
[37] J. Garcia De La Vega and B. Miguel, Orbitals expanded in slater functions with single-exponent by shell and by subshellInt. J. Quant. Chem. **51**, 397–405 (1994).
[38] K. Faegri Jr. and J. Almlöf, Energy-optimized GTO basis sets for LCAO Calculations. A Gradient ApproachJ. Comput. Chem. **7**, 396–405 (1986).